Selective hydrogenation of alkynes over ppm-level Pd/boehmite/Al2O3beads in a continuous-flow reactor

UNIVERSITÀ DEGLI STUDI DI TORINO

Selective hydrogenation of alkynes over ppm-level Pd/Boehmite/Al_2O_3 beads in a continuous-flow reactor

Zhilin Wu,[a] Emanuela Calcio Gaudino,[a] Maela Manzoli,[a] Katia Martina,[a] Maxime Drobot,[b] Ulrich Krtschil[c] and Giancarlo Cravotto[a]†

A ppm-level Pd/Boemite catalyst has been prepared over 3-mm alumina beads and used for the selective hydrogenation of alkynes in a continuous-flow reactor with two modes: closed-loop and flow-through. The flow rates of the alkyne solution and hydrogen gas are critical factors in the control of conversion and selectivity. In closed-loop mode, over 90% selectivity to alkene was achieved at over 90% conversion of phenylacetylene (PA) and 2-butyne-1,4-diol (ByD) in closed-loop mode, whereas diphenylacetylene (DPA) gave only 83% selectivity to (Z)-stilbene. The maximum outputs obtained for the hydrogenations of 22 mM PA, DPA and ByD at 60 °C, with 10 vol.% H_2 gas bubble at atmospheric pressure in the concurrent flow, were 37.8, 37.5 and 47.0 mmol min^{-1} .g^{-1} Pd, respectively. In flow-through mode, the optimal H_2 flow percentage in the concurrent flow was 44-45 vol.%, while the optimal H_2/ByD molar ratio was 1.6-1.7 for both concurrent flow rates of 0.4 and 0.7 mL min^{-1}. 90% selectivity to 2-butene-1,4-diol was achieved at over 90% ByD conversion. The maximum output was 25.2 mmol min^{-1} .g^{-1} Pd. Palladium leaching from the catalyst was evaluated in *n*-hexane and ethanol under the flow conditions over 100 hours of hydrogenation.

Introduction

Catalytic heterogeneous hydrogenation processes are arguably among the most valuable synthetic transformations known to chemists.[1] Improvement of the selective hydrogenation of alkynes, aiming to produce mainly semi-hydrogenated products (alkenes) and avoiding the formation of fully-hydrogenated products (alkanes), was done by trying new catalysts,[2,3] and reaction technologies. Since the invention of the Lindlar catalyst,[4,5] a large number of heterogeneous catalysts have been designed for selective hydrogenation[6–9], including Pd and Ag dispersed on Al_2O_3,[10] Pd–Ag/SiO_2,[11] TiO_2-modified Pd,[12] Pd–Cu alloy,[13] PdGa and Pd_3Ga_7.[14]

The partial solubility of H_2 in conventional liquid phase hydrogenation reactions can be rate limiting. High H_2 pressures and long reaction times are therefore often required to achieve high levels of conversion,[15] making special safety precautions particularly important during large scale production. Additionally, these reactions are exothermic in nature and require effective heat removal.[1] In order to overcome these limitations,[16–18] the design of highly efficient reactors with non-conventional energy sources and solvents, such as microwave,[19] ultrasound,[20] $scCO_2$,[21] and slurry, fluidized and fixed-bed flow reactors has been gradually receiving attention.[22] J. Kobayashi et al. have demonstrated an efficient system for triphase reactions using a microchannel reactor. In their work, Pd was immobilized on the inner surface of the channel where the hydrogenation reactions were smoothly conducted to quantitatively produce the desired products in 2 minutes for a variety of substrates, including diphenylacetylene and 3-phenyl-2-propyn-1-ol. Efficient interactions between hydrogen, the substrates and the palladium catalyst were achieved using extremely large interfacial areas and thanks to the short path required for molecular diffusion in a very narrow microfluidic

channel. The volumetric yield was 140,000 times higher than that produced in ordinary laboratory flasks.[15]

The microchannel technology not only improves the process economics of heterogeneous catalysis, but also provides product flexibility.[1] The high throughput and increased safety provided by the micro-volumes make continuous flow technology an especially attractive alternative to batch processing. Furthermore, improved mass and heat transfer mean that hydrogenation can be performed efficiently in a continuous flow system.[21] Besides classical chip-/plate-based microreactors, larger tubular/capillary reactors have also been employed for flow hydrogenation chemistry, including systems fitted with polytetrafluoroethylene capillaries, and stainless steel tubes. So-called trickle-bed and packed bubble-column reactors have been used for large scale-hydrogenations with liquids and gases going through the catalyst at the same time. Continuous-flow system hydrogenations have recently been attempted in fixed-bed reactors, including a ≤ 1-mm ID wall-coated capillary based system, which has performed reactions with 0.02–5.7 wt% Pd/γ-Al_2O_3,[23,24] 5 wt% Pd/C,[25] and 1 wt% Pd/θ-Al_2O_3.[26] Also, a ≥ 3-mm ID column mesoreactors has been packed with 0.67 wt% Pd/borate monolith,[27] 1 wt% Pd/Al_2O_3,[28] either 5-20 wt% CeO_2/TiO_2, Al_2O_3 or ZrO_2[29] and 5-10 wt% Pd/C [30–33] for hydrogenation reactions. Moreover, a 0.6/1.59-mm Tube-in-Tube reactor with gas-permeable Teflon AF-2400 membrane has been used for hydrogenation.[34]

Wall-coated capillary microreactors[35] and column mesoreactors[36] have several advantages, such as facile automation, secured reproducibility, improved safety and process reliability, improved mass and heat transfer and controlled residence time, which lead to superior product selectivity and high space-time yield. Furthermore, more efficient energy use can be attributed to better control of temperature, time, reagent and solvents amounts, as well as efficient mixing, while intensified processes can be achieved by applying the numbering-up and scaling-out principles.[1,36,37]

Many of these approaches use immobilized catalysts, which are embedded in a structured flow-through reactor.[38] As seen above, the palladium content in immobilized catalysts can be as high as 10%, however, little is known about the effects of ppm-level Pd catalyst on selective hydrogenation of alkynes. Palladium is a noble metal and its numerous applications and limited supply have meant that reducing Pd content in catalysts is of economic significance. In this study, the selective hydrogenation of alkynes, phenylacetylene (PA), diphenylacetylene (DPA) and 2-butyne-1,4-diol (ByD), over ppm-level Pd/Boehmite/Al_2O_3 beads has been conducted in a continuous-flow column reactor, so that the conversion of alkynes, selectivity to alkene and hydrogenation activity could be explored.

Experimental

Catalyst preparation and characterization

Boehmite (γ-AlO(OH)•nH_2O, 60% Al_2O_3, Wako Pure Chemicals Ind., Ltd.) is mainly composed of non-uniform spheroid particles in a size range of 0.78-75 μm and a D50 of 6 μm. The $Pd_{Lv\text{-}us}$/Boehmite catalyst was prepared via the ultrasound-assisted, one-pot dispersion and reduction of $Pd(OAc)_2$ (Alfa Aesar, 99%), within a Luviquat™ aqueous solution (Sigma-Aldrich, 30%). The details of the catalyst preparation and characterization methods are described elsewhere.[39] Pd content in the $Pd_{Lv\text{-}us}$/Boehmite was measured to be 0.47 wt.%

according to ICP-OES analysis. BET surface area, total volume of pores and average pore size were measured as 158 m^2 g^{-1}, 0.332 cm^3 g^{-1} and 8.4 nm, respectively, via nitrogen physisorption analysis. TEM characterization was performed by using a JEOL 2010 High Resolution Transmission Electron Microscope equipped with an Oxford Instruments Energy Dispersive X-ray Microanalysis System. Pd particle size distribution was obtained by counting a statistically representative number of crystallites (more than 200 nanoparticles) and the mean particle diameter (d_m) was calculated as $d_m = \Sigma d_i n_i / \Sigma n_i$, where n_i was the number of particles of diameter d_i. The results are shown in Figure 1, where Pd nanoparticles agglomerate well contrasted with respect to the Boehmite support were clearly detected (a,b). Interestingly, such agglomerates seem preferentially located in the macropores of the material (b).

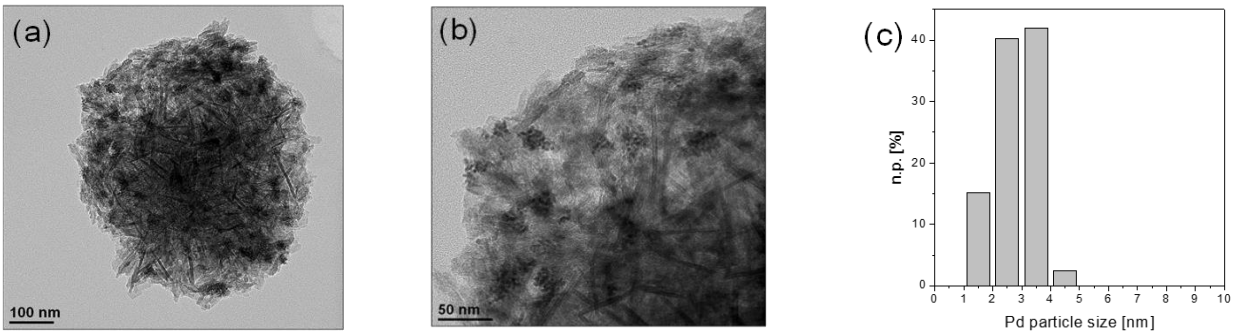

Fig. 1 TEM images of PdLv-us/Boehmite (a and b) and Pd particle size distribution (c).

Pd nanoparticles have roundish shape, with an average diameter equal to 2.8 ± 0.6 nm, as revealed by the Pd particle size distribution reported in Figure 1c. 3-mm alumina beads were then coated with this superior $Pd_{Lv\text{-}us}$/Boehmite catalyst with the help of polyvinylalcohol and glacial acetic acid in aqueous solution. The Pd content of the Pd/Boehmite/Al_2O_3 was measured to be 88 (w/w) ppm using ICP-OES. From a sustainability point of view, such value is remarkably lower than that reported in many published works assessing alkyne hydrogenation where typical catalysts have 1 wt.% (or more) of palladium.[23-33] To our knowledge, this is the first example of heterogeneous catalyst containing such a low amount of Pd. The prepared Pd catalyst is shown in Figure 2(a). The grey layers indicate that the $Pd_{Lv\text{-}us}$/Boehmite catalyst is covering the alumina beads. Figure 2(b) shows the catalyst in the column reactor.

In order to investigate the interaction between the alumina beads and the $Pd_{Lv\text{-}us}$/Boehmite catalyst, a morphological characterization was carried out by Scanning Electron Microscopy (SEM) using a ZEISS EVO 50 XVP microscope with LaB_6 source, operating at 10 kV and equipped with detectors for secondary electron as well as back scattered electron collection. Prior to examination, the sample was sputtered with a gold layer (ca. <10 nm thickness, Baltec SCD050 sputter coater).


(a)

(b)

Fig. 2 $Pd_{Lv\text{-}us}$/Boehmite coated on 3-mm alumina beads (Pd/Boehmite/Al_2O_3) (a) catalyst appearance, (b) catalyst filled in the column reactor.

The gold coating thickness had no influence on the performed measurements. It was chosen to collect the SEM images by means of the signal coming from the back scattered electrons to enhance the contrast between Pd and the alumina surface. Such approach allowed to identify those regions in which the Pd nanoparticle agglomerates (which appear white on the grey Boehmite/alumina surface) were present. SEM analysis at low magnification put in evidence that the surface of the bead is rough, made of small alumina particles, as shown in Figure 3a, and that these particles look decorated after the insertion of the $Pd_{Lv\text{-}us}$/Boehmite catalyst (Figure 3b). Indeed, a closer inspection of the surface at high magnification revealed the presence of Pd agglomerates (white points, whose composition is shown by the EDX spectrum reported in Figure 3c) located at the surface of the decorated particles (grey zones). Moreover, several EDX spot measurements were performed on different regions of the bead surface revealing a Pd amount ranging from 0.05 to 0.20 %.
Such results indicate that the very low amount of Pd contained in the catalyst is quite dispersed on the surface of the bead, even if not in a perfectly homogeneous distribution.

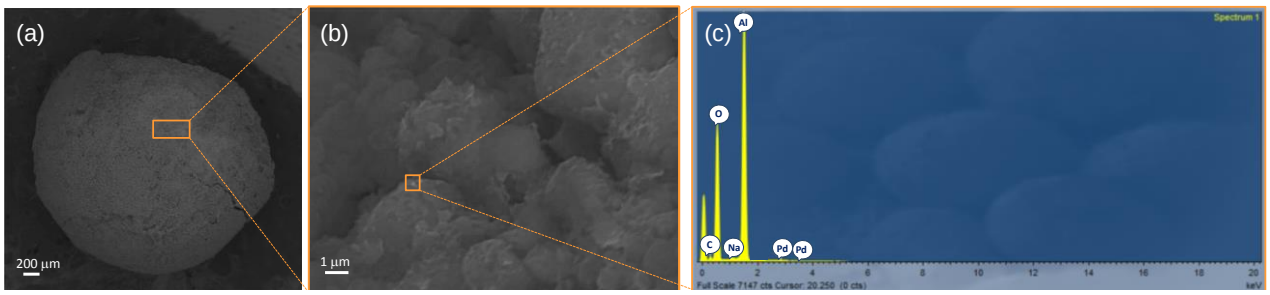

Fig. 3 SEM images of $Pd_{Lv\text{-}us}$/Boehmite layered on an alumina bead (a); enlargement of the surface of the bead (b) and EDX spectrum of the white point in the orange box (c). Instrumental magnification 60× and 18,000×, respectively.

Setup for hydrogenation

The setup for hydrogenation consisted of a Syrris Asia Syringe Pump, a Syrris Asia Heater, a RBF used as gas/liquid mixer and 7 flow-control adapters, as shown in Figure 4. The setup can operate in small-scale synthesis mode where reagents can automatically be injected

through sample loops. All the wet parts of the system are chemically resistant (PTFE, other fluorinated polymers and glass) and are rated to 20 bar (300 psi).[40]
The pump used offers two independent flow channels each with an integrated pressure sensor and a flow rate range from 1.0 µl to 2.5 ml min^{-1}. The mixed hydrogen–alkyne solution stream (concurrent flow of gas/solution), which can be controlled quickly and monitored easily using the front panel, is pumped into a column reactor. The concurrent flows of gas and liquid are driven through a gas/liquid mixer to ensure efficient gas dispersion. The flow of the substrate solution (liquid flow) was precisely metered by collecting solution in sampling vials over a period of time. Commercially available hydrogen was used as received and the hydrogen pressure in the hydrogen balloon approximately equalled atmospheric pressure. The flow of hydrogen gas bubbles (H_2 flow) in the total flow was adjusted using flow-control adapter 4 and calculated from the difference between total flow and liquid flow.
The heater used provides heating for a 3 phase reactor and can be accurately manually controlled and monitored from its front panel. Heterogeneous catalysts can be heated up to 150 °C in high temperature column reactors. In this study, either 1 g or 3.14 g Pd/Boehmite/Al_2O_3 catalysts were placed into a glass column reactor (10 mm inner diameter × 100 mm height, Figure 2), which was heated to 60 °C using an Asia Heater fitted with a column adaptor. The column reactor was connected to the pump in a top-down arrangement and either the gas-liquid mixer or sampling vials via PTFE tubes (Figure 4). At the reactor outlet, the product solution was either introduced into the gas/liquid mixer in closed-loop mode or collected in the sampling vials within the flow-through mode.

Hydrogenation of alkynes

In order to investigate the effects of flow conditions on the hydrogenation of alkynes (98% PA, Alfa Aesar ; 99% DPA, Alfa Aesar; 98% ByD, Alfa Aesar), this continuous-flow system was designed to be configurable to either closed-loop mode or flow-through mode by switching flow-control adapter 1.
Hydrogenation in closed-loop mode. In a typical run, 1 g of 88-ppm Pd/Boehmite/Al_2O_3 catalyst was placed in the column reactor and initially washed with 20 mL *n*-hexane (Sigma-Aldrich, ≧99%), at a flow rate of 1.0 mL min^{-1} for ca. 20 min in flow-through mode. 50 mL of a 11 mM PA solution in *n*-hexane was then allowed to flow through the fixed bed at a constant flow rate of 1 mL min^{-1} for 10 min and the effluent was collected in the sampling vials. The last ca. 1.0 mL of effluent was collected and analysed as the starting sample. The volume of the remaining solution for hydrogenation was thus 40 mL after washing. The reaction system was closed by switching flow-control adapters 1 and 3, and then purged using a vacuum pump which provided a vacuum of -0.08 MPa. Nitrogen (Sapio, grade 6.0) from a connected N_2 balloon was used to flush the system before the reaction system was purged under vacuum again.

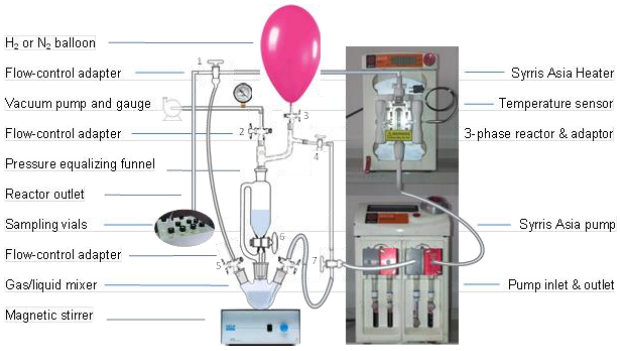

Fig. 4 Continuous flow hydrogenation setup

Finally, the closed system was filled with hydrogen (Sapio, grade 4.5) via the connected H_2 balloon. The reactor temperature and rotation speed of the gas/liquid mixer were set at the values indicated. The concurrent streams of H_2 bubbles and the PA solution were then allowed to flow into the column reactor at room temperature and the effluent from the column reactor was introduced into the gas/liquid mixer via the flow-control adapter 1. Thus, 40 mL of 11 mM PA solution was recycled under static H_2 atmosphere and the reaction ended at ca. 90% PA conversion.[41] Aliquots (1 mL) of the solution were periodically collected from the reaction system by flow-control adapter 1 and analysed using a GC/FID (Agilent Technologies 7820A GC system equipped with a G4513A sampler, a FID Detector and an HP-5 capillary column). At constant concurrent flow (2.5 mL min^{-1}), the flow rate of the 11 mM PA solution was varied between 1.75 and 2.50 mL min^{-1} by adjusting the proportion of H_2 bubbles in the concurrent flow. The flow rate of the H_2 and PA solutions, the input rate and amounts of H_2 and the ratio of H_2 and PA during hydrogenation are calculated and listed in Table 1.

Hydrogenation in flow-through mode. Most of the hydrogenation procedure was the same as in closed-loop mode. The only difference was that the effluent from the column reactor was introduced straight into the sampling vials via flow-control adapter 1. The ByD solution in ethanol (Fluka, 99.8%) was thus not recycled under the static H_2 atmosphere, but directly flowed out from the column reactor. In addition, the amount of Pd-catalyst in the column reactor was 3.14 g instead of 1 g so that higher conversions were achieved in flow-through mode. The substrate conversion rate can be controlled by adjusting the flow rate of H_2 and the solution.

Table 1. The flow rate of the H_2 and PA solutions, input rate and amounts of H_2, as well as the ratio of H_2 and PA during hydrogenation at room temperature and atmospheric H_2 pressure[42,43]

H_2 PCT, %	F_{H2}, mL min^{-1}	F_{PA}, mL min^{-1}	R_{DH2}, µmol min^{-1}	R_{BH2}, µmol min^{-1}	R_{H2}, µmol min^{-1}	t, min	M_{H2}, µmol	H_2/PA, mol/mol
0	0	2.500	13.8	0.0	13.8	90	1240	2.8
1	0.025	2.475	13.6	1.0	14.7	73	1070	2.4

2	0.050	2.450	13.5	2.0	15.5	70	1088	2.5
5	0.125	2.375	13.1	5.1	18.2	70	1274	2.9
10	0.250	2.250	12.4	10.2	22.6	70	1584	3.6
30	0.750	1.750	9.6	30.7	40.3	60	2420	5.5

Note: 11 mM PA in 40 mL *n*-hexane (440 μmol PA in solution). H_2 PCT: H_2 bubbles percentage in total flow; F_{H2}: H_2 flow rate; F_{PA}: PA-containing liquid flow rate; R_{DH2}: Input rate of dissolved H_2; R_{BH2}: Input rate of H_2 bubbles; R_{H2}: Total input rate of H_2; t: Reaction time; M_{H2}: Total input of H_2.

The initial concentrations of ByD were varied and aliquots (0.1-0.5 mL) of the solution were periodically collected by the flow-control adapter 1 from the reaction system. Subsequently, the samples were evaporated down to 0.1 mL under a flow of nitrogen and then diluted with 0.9 mL $CHCl_3$ for GC/MS analysis, which was carried out on an Agilent Technologies 6850 Network GC system equipped with a 5973 Network Mass Selective Detector and an HP-5MS capillary column with the following characteristics; 30 m length, 0.25 mm ID and 0.25 μm film thickness.

Results and discussion

Hydrogenation in closed-loop mode

In a typical closed-loop flow experiment, 11 mM PA in *n*-hexane with 2.5 mL min^{-1} of concurrent flow (inlet flow or total flow) was passed through a column reactor at 60 °C under atmospheric H_2 pressure. Alkyne conversion, selectivity to (Z)-alkene and hydrogenation activity were calculated by GC/FID analysis of the composition of the reaction mixture. The effects of reaction conditions on the selective hydrogenation of alkynes were studied by adjusting the proper settings on the instrument (H_2 and liquid flow rate, initial concentration and temperature).[31]

Effect of H_2 percentage in inlet flow. It has been shown that alkynes and alkenes can be simultaneously hydrogenerated in the presence of a large excess of hydrogen;[44] thus the H_2/alkyne ratio in the inlet flow essentially influences conversion and selectivity during the partial hydrogenation of alkynes.[45] The effect of H_2 proportion on PA hydrogenation over 1 g of 88 ppm Pd/Boehmite/Al_2O_3 was investigated under closed-loop flow conditions. Hydrogenation activity and styrene yield, determined as the product of PA conversion and styrene selectivity, are presented in Figure 5.

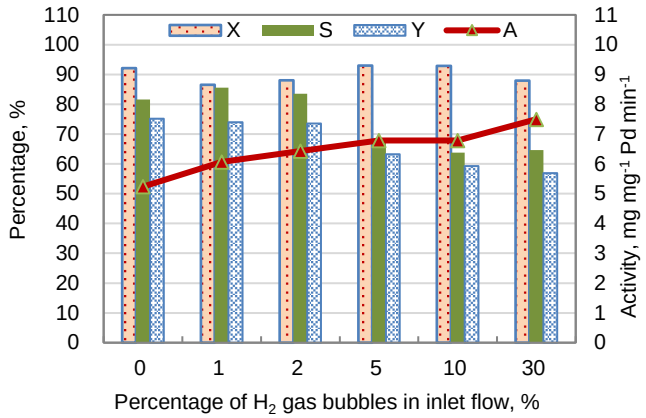

Fig. 5 The effect of the percentage of H_2 gas bubbles in the inlet flow on the conversion (X) of PA, selectivity (S) and yield (Y) to styrene and hydrogenation activity (A) over 1 g of 88 ppm Pd/Boehmite/Al_2O_3. Hydrogenation conditions: 11 mM of initial concentration of PA , 40 mL of PA solution, 60 °C of reaction temperature, 2.5 mL min^{-1} of inlet flow (H_2+PA solution) and atmospheric H_2 pressure.

40 mL of 11 mM PA in H_2-saturated *n*-hexane was recycled under a static H_2 atmosphere at a constant reaction temperature of 60 °C. As shown in Figure 5, the hydrogenation activity of PA is critically dependent on H_2 percentage in the concurrent flow. Initial studies conducted with only dissolved H_2 in the PA solution, without H_2 gas bubbles in the concurrent flow, gave relatively low PA hydrogenation activities; 5% and 30% gas bubbles of H_2 in 11 mM PA solutions resulted in 30% and 43% increases in hydrogenation activity, as typically observed in the partial hydrogenation of alkynes.[46]

The selectivity is significantly influenced by the proportion of H_2 in the inlet flow.[47] This is attributed to the rapid hydrogenation of PA under large H_2 excesses, when H_2 bubble percentages in the inlet were over 5%. Under large H_2 excesses, styrene can also be hydrogenated and the full-hydrogenated product, ethylbenezene was formed, leading to the decrease in styrene selectivity (Figure 5). The input amounts and ratios of H_2 and PA during PA hydrogenation are listed in Table 1. The dissolved amounts of H_2 in *n*-hexane were calculated using relative references.[42,43] H_2 was clearly present in large excess over PA when H_2 bubble percentages in the inlet flow were higher than 5%.

G. Vilé et al. have also reported that, at 2.5 vol % inlet alkyne concentration, propane formation was not detected in a continuous-flow fixed-bed microreactor over CeO_2 at any condition despite the large hydrogen excess in the feed (H_2/C_3H_4 ratio: 5-30). However, the conversion of propyne increases quasi-linearly upon increasing the inlet partial pressure of hydrogen, as does the selectivity to propene. These results strongly suggest that hydrogen activation on the ceria surface is the rate-limiting step.[48]

Catalytic 1-pentyne gas-phase hydrogenation was carried out on Pd black in a closed-loop circulation setup. Subsurface H strongly enhanced the total hydrogenation of acetylene, whereas surface H alone (without any subsurface population) was much more selective toward ethylene. H content was slightly higher when running unselective 1-pentyne hydrogenation (H_2/C_5>7), which means (1) that the reaction proceeds on saturated β-hydride and (2) that additional deposits and adsorbates should carry even more H. This finding validates the idea

that bulk-dissolved and subsurface H are very reactive but unselective species and, furthermore, that the equilibrium between the surface and bulk is maintained during total hydrogenation. However, hydrogenation was selective and the H/Pd ratio was low (0.15 on average), when 1-pentyne was hydrogenated at low H_2/C_5 ratios (<5), after room-temperature H_2 pre-treatment. H dissolution would appear to be more favourable at slightly lower temperatures and shifts selectivity to favour alkanes again.[49]

Effect of initial alkyne concentration. Higher selectivity towards styrene was achieved at a higher initial PA concentration (22 mM), even under large H_2 input excess, as shown in Table 2. This behaviour is attributed to the PA over-layer present on the working catalyst that exposes the metal sites.[46]

Table 2 Comparison of conversion of PA, selectivity and yield to styrene between 11 and 22 mM PA over 1 g of 88 ppm Pd/Boehmite/Al_2O_3

	11 mM PA				22 mM PA			
H_2 PCT	H_2/PA,	X, %	S, %	Y, %	H_2/PA,	X, %	S, %	Y, %
1	2.4	86.5	85.5	74.0	3.2	96.7	87.4	84.5
5	2.9	93.0	68.1	63.0	3.9	87.1	94.5	82.3
10	3.6	92.9	63.8	59.0	4.9	89.7	91.9	82.4

Note: Hydrogenated conditions: 40 ml of PA solution; 880 µmol of PA mass; 2.5 mL min^{-1} of total flow (H_2 + PA Solution); 60 °C of reaction temperature and atmospheric H_2 pressure. H_2 PCT: H_2 bubbles percentage in total flow; X: PA conversion; S: selectivity to styrene; Y: yield to styrene.

TA Nijhuis et al., have reported that the initial concentration of 3-methyl-1-pentyn-3-ol has a strong influence on the maximum yield (%) of the desired alkene. The alkyne zero order reaction can be explained in terms of alkyne adsorption, which is much higher than the adsorption of alkene and alkane, resulting in the catalyst surface being essentially completely occupied by the alkyne which therefore reacts at a constant rate. Moreover, under a high initial alkyne concentration, the reaction is hydrogen-limited on the catalyst particles, and the alkyne and alkene react according to their kinetic preference. Additionally, the reaction is further limited by the diffusion of organic molecules inside catalyst particles and over hydrogenation can occur more easily, explaining the lower selectivity.[50]

During the selective hydrogenation of ethyne to ethene over a Pd catalyst, high selectivity can be maintained, as long as some ethyne is present, even with excess hydrogen in a constant volume system. When all of the ethyne has reacted, ethene then hydrogenates quicker, which reduces selectivity.[44]

In this study, a longer reaction time was needed when increasing the initial concentration of PA, in order to achieve the given conversion. Fortunately, the selectivity to styrene was well maintained at the higher conversion, even with the higher H_2 flow.

Effect of liquid flow. In the closed-loop flow system, the liquid flow rate is the dominating factor for determining the residence time over the catalyst and the input amount of dissolved H_2. In order to simplify the study, the influence of the liquid flow rate on the selective hydrogenation of PA was initially studied without H_2 gas bubbles at room temperature, as shown in Table 3. The maximum rate of concurrent flow attainable through the column reactor

using the pump was 2.5 ml min^{-1}. This flow rate was high enough to produce very low alkyne conversion per pass.[51]

As shown in Table 3, all PA conversions within the closed-loop flow reactor were around 90% with dissolved hydrogen when the reaction time was ca. 300 min at room temperature, except at the very low liquid flow rate (0.5 mL min^{-1}). High selectivity to styrene was also achieved, resulting in almost equal yields of styrene. Increasing the liquid flow rate generally decreased the residence time over the catalyst,

Table 3 Effects of liquid flow on the selective hydrogenation of PA over 1 g of 88 ppm Pd/Boehmite/Al_2O_3

Entry	$F_{PA,}$ mL min^{-1}	R_{DH2}, µmol min^{-1}	t, min	M_{H2}, µmol	H_2/PA, mol/mol	N_{pass}	T_R/pass, s	T_R, min	X, %	S, %	Y, %	A, mg^{-1} mg Pd min^{-1}	X/pas, %
1	0.5	2.8	360	992	2.3	4.5	90	6.8	79.7	96.4	77	1.13	17.7
2	1.0	5.5	300	1653	3.8	7.5	45	5.6	90.4	92.9	84	1.54	12.1
3	1.2	6.6	300	1984	4.5	9.0	38	5.6	96.2	84.9	82	1.64	10.7
4	1.4	7.7	235	1813	4.1	8.2	32	4.4	92.9	89.2	83	2.02	11.3
5	1.6	8.8	235	2072	4.7	9.4	28	4.4	95.1	87.1	83	2.07	10.1
6	1.8	9.9	180	1785	4.1	8.1	25	3.4	91.0	89.0	81	2.59	11.2
7	1.8[a]	9.9	124	1230	2.8	5.6	25	2.3	90.2	89.2	80	3.72	16.1
8	2.5[a]	13.8	90	1240	2.8	5.6	18	1.7	92.2	81.6	75	5.23	16.5
9	1.8[b]	9.8	95	1003	2.3	4.2	25	1.8	87.3	85.9	75	4.70	20.8
10	2.5[b]	13.6	73	1070	2.4	4.5	18	1.4	86.5	85.5	74	6.06	19.2
11	2.5[c]	13.6	125	1833	4.2	7.7	18	2.3	92.4	80.7	75	3.78	12.0

Note: Conditions: 11 mM PA in *n*-hexane, dissolved H_2 without gas bubbles in inlet under atmospheric H_2 pressure and at room temperature without special notes. (a) without H_2 gas bubble in inlet at 60 °C, (b) with 1% H_2 gas bubbles in inlet at 60 °C, (c) with 1% H_2 gas bubbles in inlet at 25 °C. R_{DH2}: Input rate of dissolved H_2; F_{PA}: PA-containing liquid flow rate; t: Reaction time; M_{H2}: Total input of H_2; N_{pass}: Circulation pass number; T_R: Residence time; X: PA conversion; S: selectivity to styrene; Y: yield to styrene; A: hydrogenation activity.

but increased the input rate of H_2 during hydrogenation and consequently increased PA hydrogenation activity. When the liquid flow rate reached 1.4 mL min^{-1}, the relatively violent turbulence might promote contact between PA, H_2 and catalyst, leading to higher activity.

Thus the input amount and phase transfer of H_2 rather than residence time thus dominated PA hydrogenation activity, but had little effect on selectivity to styrene. G. Vilé et al. reported that propyne conversion doubles when residence time increases from 0.08 to 0.21 s, while propene selectivity is practically unchanged. In the same work, they also deposited minute amounts of palladium (0.05 wt % Pd) onto CeO_2 and evaluated its performance in propyne hydrogenation. However, the undesired fully hydrogenated product (propane) was obtained under the optimal conditions identified for ceria with selectivity exceeding 95 %.[48]

The hydrogenation activity of PA at 60 °C was much higher under 2.5 mL min^{-1} of concurrent flow rate than 1.8 mL min^{-1}, regardless of the presence or absence of H_2 gas bubbles, as seen in entries 7, 8 and 9, 10 in Table 3. However, the conversion per pass and the circulation pass number at 90% conversion were not affected by the concurrent flow rate. Thus, an equal H_2 input amount was required to achieve about 90% PA conversion at 60 °C, while the selectivity to styrene was significantly lower at higher concurrent flow rates than that at lower concurrent flow. This indicates that the PA layer over the catalyst was destroyed under higher concurrent flow as the temperature was sufficiently high.

The hydrogenation rate increased with increasing flow of PA solution, which is due to the higher pass through the reactor and H_2 input at higher liquid flow rates. Selectivity to the semi-hydrogenated product decreased when increasing liquid flow rate, but ca. 90% PA conversion was maintained at any liquid flow rate.

Effect of temperature. The selective hydrogenation of 11 mM PA in 40 mL *n*-hexane was studied over 1 g of 88 ppm Pd/Boehmite/Al_2O_3 with a H_2 gas balloon at both 25 and 60 °C. The concurrent flow rate was 1.8 mL min^{-1} in the absence H_2 gas bubbles and 2.5 mL min^{-1} in the presence 1% H_2 gas bubbles. The influence of temperature on hydrogenation and the reaction conditions are summarized in entries 6, 7, 10 and 11 in Table 3. With identical feed PA concentration and inlet flow rate, the reaction times to achieve 90% conversion were shortened by 31-42% at 60 °C as compared to room temperature reactions. This indicates that the higher activity of PA hydrogenation at 60 °C led to less circulation pass, shorter residence time over the catalyst, lower H_2 input amount and H_2/PA ratio. Increasing the temperature did not significantly decrease selectivity to styrene, leading to similar styrene yields being achieved at a variety of temperatures.

JA Alves et al. have reported that hydrogen partial pressure (0.8 to 8 atm) is a crucial operating variable, whereas temperature level (27 and 62 °C) does not have a significant effect on process selectivity during the hydrogenation of 0.6 M 1-butyne over a commercial palladium-based catalyst.[51] D. Teschner et al. have also reported that rising temperature promotes hydrogenation rate and does not attenuate selectivity. The population, by either hydrogen or carbon, of palladium subsurface sites thus governs the hydrogenation events on the surface.[49] By contrast, G. Vilé et al. have reported that propene selectivity strongly decreases with temperature, from 91 % at 523 K to 25 % at 673 K, during the hydrogenation of propyne.[48] Selectivity to the alkene product over the c-Pd catalysts only drops when higher temperatures (293-353 K) and pressures (1–9 bar) are applied.[28]

The state of Pd depended strongly on reaction temperature, when the concentration of H_2 in the gas phase was near the limit of the phase transition of Pd to Pd β-hydride. PdC appeared substantially above the decomposition temperature of β-hydride. Bulk dissolved H, which is much more energetic than adsorbed surface H, can hydrogenate surface adsorbates upon emerging to the surface.[49] This is possible in the region of room temperature, while higher temperatures encouraged the simultaneous formation of alkenes. When this occurred, the two processes occurred in parallel. However, selectivity remained constant while any alkynes were still present. The β-PdH phase is stable at higher temperatures during ethyne hydrogenation, while the β-PdH to α-PdH transition considerably increases ethene selectivity at lower C_2H_2 partial pressure (3.16 kPa) and lower temperature (300 K).[44] In this study, higher temperatures, in the range of 25-60 °C, promoted the alkyne hydrogenation rate, but did not reduce selectivity to alkenes.

Comparison of PA, DPA and ByD hydrogenation. Alkyne conversion, selectivity, yield to (Z)-alkene and PA, DPA and ByD hydrogenation activity are compared and results are listed in Table 4. 2.5 mL min^{-1} inlet flow, made up of 0.25 mL min^{-1} H_2 gas bubble flow (10% of H_2 gas bubbles in inlet flow) and 2.25 mL min^{-1} alkyne-containing liquid flow, passed the column reactor containing 3.14 g of catalyst beads. The total input rate of H_2 was thus 22.6 µmol min^{-1}, of which dissolved H_2 and H_2 in gas bubbles were 12.4 and 10.2 µmol min^{-1}, respectively. Using 40 mL of a 22 mM alkyne solution, the input rate and amount of alkyne were calculated to be 49.5 µmol min^{-1} and 880 µmol, respectively. The residence time over the catalyst was calculated to be 63 s per pass based on a liquid space between catalyst beads of 2.355 mL and an alkyne-containing liquid flow rate of 2.25 mL min^{-1}.

As listed in Table 4, where hydrogenation activity is represented as the conversion of molar units (amount of moles per unit time and unit amount of catalyst), the ByD hydrogenation gave higher activity than PA and DPA hydrogenation. PA and DPA gave similar activity, as higher alkyne polarity provides better compatibility with Pd/Bohmite/Al_2O_3. Higher activity, a lower H_2/ByD ratio, a lower circulation pass number and shorter total residence time over the catalyst all contributed to the higher selectivity to (Z)-2-Butene-1,4-diol (BeD) in the ByD hydrogenation.

Figure 6 shows the relationship between alkyne conversion and selectivity to (Z)-alkene for PA, DPA and ByD hydrogenation at 60 °C and atmospheric H_2 pressure. As shown in Figure 6, selectivity to (Z)-alkene decreased with increasing alkyne conversion and was higher (>90 %), even at >90 % conversion for PA and ByD hydrogenation. However, selectivity to Z-stilbene was only 83% at 92% DPA conversion and selectivity further dropped to 80% at 94% DPA conversion. Although 83% selectivity to Z-stilbene in this closed-loop system was slightly lower than the ca. 88% selectivity obtained with the batch reactor in our previous study,[39] selectivity of up to 85% to Z-stilbene has been reported as being high for DPA hydrogenation in other previous studies.[52–54]

Table 4 Comparison of the conversion, selectivity, yield and activity of PA, DPA and ByD hydrogenation

Alkyne	t, min	pass	M_{H2}, µmol	H_2/PA, mol/mol	T_R min	X, %	S, %	Y, %	X/pass, %	A, mg/mg Pd min	A_{mol}, mmol g^{-1} Pd min^{-1}
PA	80	4.5	1808	2.1	4.7	94.0	93.2	87.7	20.9	3.86	37.8
DPA	80	4.5	1808	2.1	4.7	93.5	79.5	77.0	20.8	6.68	37.5
ByD	65	3.7	1469	1.7	3.9	94.6	91.4	86.5	25.9	4.05	47.0

Note: Hydrogenation conditions: 22 mM PA or DPA in *n*-hexane, 22 mM ByD in ethanol (99%); 3.14 g of 88 ppm Pd/Boehmite/Al_2O_3; 40 mL of solution; 880 µmol of alkyne mass; 2.5 mL min^{-1} of inlet flow; made up of 0.25 mL min^{-1} of H_2 gas bubble flow and 2.25 mL min^{-1} of alkyne-containing liquid flow; 60 °C of reaction temperature and atmospheric H_2 pressure. t: Circulation time; M_{H2}: Total input of H_2; T_R: Residence time, X: alkene conversion, S: selectivity to (Z)-alkene, Y: yield to (Z)-alkene, A: hydrogenated activity

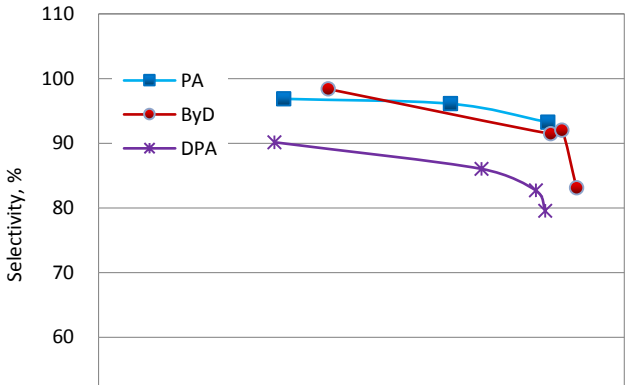

Fig. 6 Selectivity to (Z)-alkenes over 3.14 g of 88 ppm Pd/Boehmite/Al_2O_3 as a function of alkyne conversion. Hydrogenation conditions: 22 mM of initial concentration of alkyne; 40 mL of solution; 2.5 mL min^{-1} of inlet flow; 10% H_2 gas bubbles in inlet; 60 °C of reaction temperature and atmospheric H_2 pressure.

It is not entirely clear why DPA hydrogenation displayed slightly lower selectivity to Z-stilbene than PA hydrogenation. A likely explanation is the formation of semi-hydrogenated product stereoisomers during DPA hydrogenation under these hydrogenation conditions, as selectivity to E-stilbene reached over 2% at >90 % DPA conversion.
In short, ByD hydrogenation activity is higher than those of PA and DPA. Over 90% selectivity to alkene was achieved at over 90% PA or ByD conversions, but only 83% selectivity was observed for DPA in closed-loop mode.

3.2 Hydrogenation of ByD in flow-through mode

Effect of liquid flow and H_2 flow. The concurrent flow, including the liquid flow containing 22 mM ByD in 99% ethanol and H_2 gas flow in the inlet, was set to be 0.4 and 0.7 mL min^{-1}. The glass column reactor was filled with 3.14 g of 88 ppm Pd/Boehmite/Al_2O_3 catalyst.
The liquid space between catalyst beads (2.355 mL) as well as the H_2 and liquid flow in the inlet were used to calculate the H_2 percentage in the concurrent flow, input rate of H_2 and ByD, the ratio of H_2/ByD and the residence times with catalyst. These data are listed in Table 5.
In closed-loop mode, a 94.6% conversion of 40 mL of 22 mM ByD was achieved after 65 min at 60 °C and atmospheric H_2 pressure. Total residence time over the catalyst was calculated to be 3.9 min when 90% of ByD conversion was achieved (Table 4), indicating that over 3.9 min of residence time for one pass in flow-through mode is theoretically required to achieve over 90% conversion under the same dynamic conditions. Figure 7 shows the conversion and selectivity obtained from 22 mM ByD hydrogenation through 3.14 g Pd/Boehmite/Al_2O_3 beads at 60 °C and atmospheric H_2 pressure in flow-through mode.
Table 5. H_2 percentage in concurrent flow, input rate of H_2 and ByD, H_2/ByD ratio and the residence times on the catalyst in flow-through mode

Total flow	F_{ByD}, mL min^{-1}	F_{H2}, mL min^{-1}	H_2 PCT, %	R_{DH2}, µmol min^{-1}	R_{BH2}, µmolmin^{-1}	R_{H2}, µmol min^{-1}	R_{ByD}, µmol min^{-1}	H_2/ByD, mol/mol	t, min
0.4	0.06	0.34	85	0.2	13.9	14.1	1.3	10.7	39.3

mL min^{-1}	0.09	0.31	78	0.3	12.7	13.0	2.0	6.6	26.2
	0.11	0.29	73	0.4	11.9	12.3	2.4	5.1	21.4
	0.15	0.25	63	0.5	10.2	10.8	3.3	3.3	15.7
	0.16	0.24	60	0.6	9.8	10.4	3.5	3.0	14.7
	0.18	0.22	55	0.6	9.0	9.7	4.0	2.4	13.1
	0.20	0.20	50	0.7	8.2	8.9	4.4	2.0	11.8
	0.22	0.18	45	0.8	7.4	8.2	4.8	1.7	10.7
	0.24	0.16	40	0.9	6.5	7.4	5.3	1.4	9.8
0.7 mL min^{-1}	0.31	0.39	56	1.1	16.0	17.1	6.8	2.5	7.6
	0.35	0.35	50	1.3	14.3	15.6	7.7	2.0	6.7
	0.38	0.32	46	1.4	13.5	14.9	8.4	1.8	6.2
	0.39	0.31	44	1.4	12.7	14.1	8.6	1.6	6.0
	0.40	0.30	43	1.4	12.3	13.7	8.8	1.6	5.9
	0.45	0.25	36	1.6	10.2	11.9	9.9	1.2	5.2
	0.48	0.22	32	1.7	9.4	11.1	10.6	1.1	4.9
	0.50	0.20	29	1.8	8.2	10.0	11.0	0.9	4.7
	0.55	0.15	21	2.0	6.1	8.1	12.1	0.7	4.3

Note: H_2 PCT: H_2 bubbles percentage in total flow; F_{H2}: H_2 flow rate; F_{ByD}: ByD-containing liquid flow rate; R_{DH2}: Input rate of dissolved H_2; R_{BH2}: Input rate of H_2 bubbles; R_{H2}: Total input rate of H_2; R_{ByD}: Input rate of ByD; t: Residence time over catalyst.

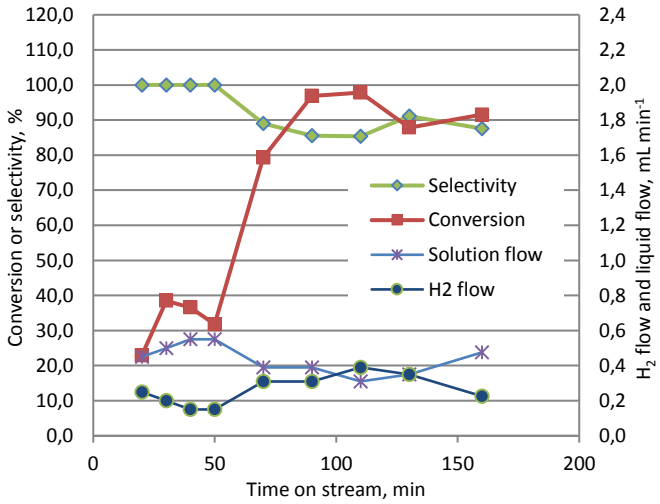

Fig. 7 ByD conversion and selectivity to BeD during the flow-through process. Hydrogenation conditions: 3.14 g of 88 ppm Pd/Boehmite/Al_2O_3; 22 mM ByD in 99% ethanol; 0.7 mL min^{-1} of inlet flow; 60 °C of reaction temperature and atmospheric H_2 pressure.

As shown in Figure 7, ByD conversion was less than 40% at 0.45-0.55 mL min^{-1} liquid flow at the beginning of hydrogenation. As the liquid flow rate dropped to 0.31-0.39 mL min^{-1}, the conversion increased to 80-98%, but selectivity to 2-butene-1,4-diol decreased from 100% to

85-89%. In order to achieve better selectivity, the liquid flow was raised to 0.35-0.48 mL min^{-1}. 88-91% selectivity was thus achieved at about 90% conversion. Under constant concurrent flow, higher liquid flow led to a lower H_2/ByD ratio and lower residence times over the catalyst (Table 5), resulting in a decrease in ByD conversion and an increase in selectivity to BeD.[41,55]

In short, ByD conversion and selectivity to BeD are dependent on liquid flow and H_2 flow in continuous flow-through mode. Lower ByD-containing liquid flow led to higher ByD conversion, but lower selectivity to BeD.

Consequently, both conversion and selectivity were controlled by regulating solution and H_2 flow rates, as shown in Figure 8.

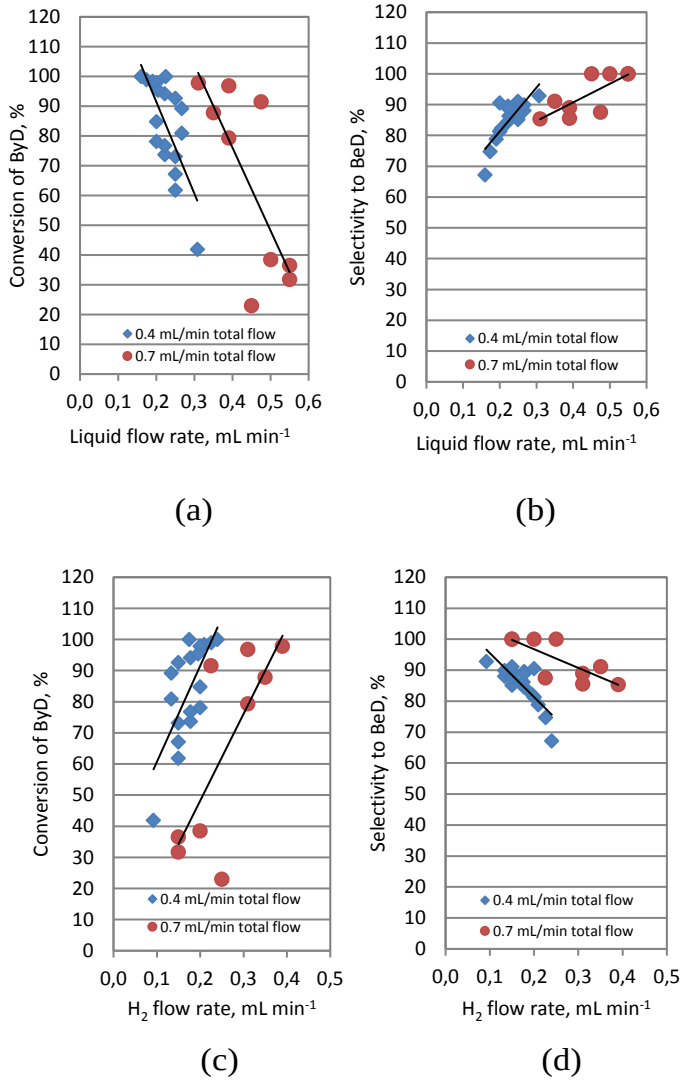

Fig. 8 Hydrogenation of 22 mM ByD in ethanol over 3.14 g of 88 ppm Pd/Boehmite/Al_2O_3 at 60 °C and atmospheric H_2 pressure in flow-through mode: (a) conversion of ByD as a function of liquid flow rate; (b) selectivity to BeD as a function of liquid flow rate; (c) conversion of ByD as a function of H_2 flow rate; (d) selectivity to BeD as a function of H_2 flow rate.

On the whole, ByD conversion significantly decreased with increasing liquid flow rate while maintaining the same concurrent flow rate because of the decrease of both the contact time over the catalyst and H_2 flow rates. However, selectivity to BeD increased with increasing

liquid flow rate at constant concurrent flow rate (0.4 or 0.7 mL min^{-1}). Meanwhile, ByD conversion increased and selectivity to BeD decreased with increasing H_2 flow rate.
Under lower concurrent flow (0.4 mL min^{-1}), the best compromise between conversion and selectivity was reached at a liquid flow rate of 0.22 mL min^{-1} and a H_2 flow rate of 0.18 mL min^{-1}, giving ca. 90% conversion and 90% selectivity. The productivity of the reaction was 14.2 mmol min^{-1} g^{-1} Pd. Under higher concurrent flow (0.7 mL min^{-1}), the best compromise between conversion and selectivity was reached at a liquid flow rate of 0.39 mL min^{-1} and a H_2 flow rate of 0.31 mL min^{-1}, giving ca. 90% conversion and 90% selectivity. The productivity of the reaction was 25.2 mmol min^{-1} g^{-1} Pd. Obviously, the hydrogenation efficiency of ByD at the higher concurrent flow rate is higher than that at the lower one. Coincidentally, the optimal H_2 flow percentage in the inlet flow was 44-45% and the optimal H_2/ByD molar ratio was 1.6-1.7 both at total flow rates of 0.4 and 0.7 mL min^{-1} (Table 5). Under optimal conditions, 90% selectivity to BeD was achieved at 90% ByD conversion, regardless of inlet flow rate and the various residence times over catalyst.[41]
Effect of initial concentration of ByD. In general, increasing the initial substrate concentration decreases the hydrogenation rate as well as the conversion for non-zero order kinetics under the same reaction conditions. As shown in Figure 9, all the conversions of 44 mM ByD were lower than 70% at higher than 0.11 mL min^{-1} liquid flow rate, unless it was very low (e.g. 0.06 mL min^{-1}). In this case, the residence time over the catalyst reached 39.3 min and the H_2/ByD molar ratio reached 10.7 (Table 5), leading to 96.5% ByD conversion, but low selectivity to BeD (67.7%). The productivity of the reaction was 6.23 mmol min^{-1} g^{-1} Pd.

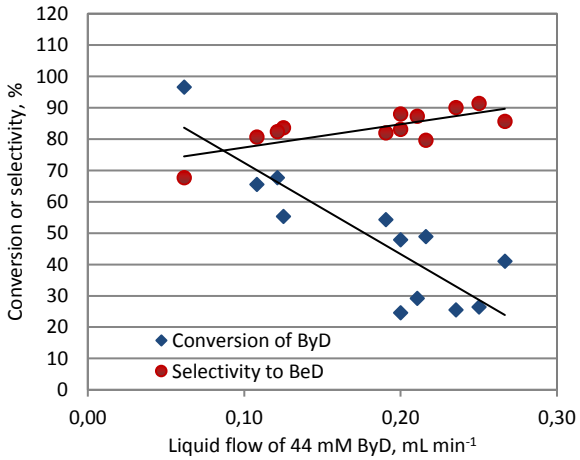

Fig. 9 Conversion and selectivity during the hydrogenation of 44 mM ByD in ethanol (0.4 mL min^{-1} inlet flow) over 3.14 g of 88 ppm Pd/Boehmite/Al_2O_3 at 60 °C and atmospheric H_2 pressure in flow-through mode.

However, 100% conversion of 22 mM ByD and 67.2% selectivity to BeD were achieved at 0.16 mL min^{-1} liquid flow rate, which led to a residence time over catalyst of 14.7 min and a H_2/ByD molar ratio of 3.0 (Table 5). The productivity of the reaction was 8.6 mmol min^{-1} g^{-1} Pd. In comparison, the same conversion, at a higher initial substrate concentration (e.g. 44

mM ByD), can be achieved at very low liquid flow rates and at higher H_2/ByD molar ratios for longer residence times over the catalyst.[27]

As the initial concentration of ByD further increased to 88 mM, maximum ByD conversion only reached 42% under the presently available flow-through conditions, as shown in Figure 10. Increasing the Pd content in the catalyst is obviously the most effective approach. Selectivity to BeD as a function of ByD conversion in ethanol over 3.14 g of 88 ppm Pd/Boehmite/Al_2O_3 at 60 °C and atmospheric H_2 pressure in flow-through mode is shown in Figure 10. Selectivity decreased upon increasing ByD conversion, especially over 90% conversion, regardless of initial substrate concentration. However, over 80% of selectivity to BeD was easily achieved at over 90% conversion by controlling liquid flow rate at a constant concurrent flow rate.

Note that ethanol was substantially used as solvent for the polar substrate, but it has been demonstrated that ethanol can also act as a hydrogenating agent for ynamides under palladium catalysis.[56] The reaction shows stereoselectivity for E-enamides, which is in contrast to reports using other hydrogenating sources.

Leaching test under the flow conditions. A leaching test of Pd/Boehmite has been conducted both under sonication and stirring. The digested sample and analytic method were reported in our previous study.[20] The results showed no metal leached from the Pd/Boehmite catalysts during sonication, but Boehmite particles were cracked into finer particles by sonication, indicating that Pd/Boehmite is quite robust in hexane and ethanol. The removal of metal from the catalysts during sonication is due to the fragmentation that was caused by the implosion of cavitation bubbles near the surface, possibly leading to the formation of nanoparticles, rather than leaching through the formation of soluble metal compounds.

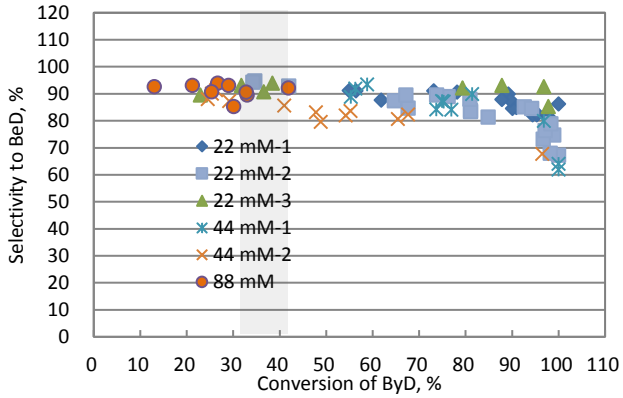

Fig. 10 Selectivity to BeD as a function of ByD conversion in ethanol over 3.14 g of 88 ppm Pd/Boehmite/Al_2O_3 at 60 °C and atmospheric H_2 pressure in flow-through mode.

The stability of the Pd/Boehmite/Al_2O_3 catalyst proved remarkable as both conversion and selectivity were nearly constant over a period of 100 h. Pd content in the solution was below the detection limit of the ICP-OES instrument, i.e. 0.006 ppm, during the entire reaction, indicating that Pd loss is negligible even after 100 h time-on-stream.

However, Pd content in the non-used Pd/Boehmite/Al_2O_3 catalyst was measured to be 88 ppm and became 68 ppm after 100 h running, meaning that 22.7% Pd was transferred from the

alumina beads to powder during the continuous flow runs. This indicates that some Pd/Boehmite powder had fallen from the catalyst but stayed in the column reactor.

Conclusions

In conclusion, a new Pd/Boehmite/Al_2O_3 bead catalyst containing highly dispersed Pd nanoparticles at ppm-level has been effectively synthesized. Such system has been evaluated in a continuous flow system for the selective hydrogenation of alkynes. Both closed-loop and flow-through modes have been conducted successfully on the Syrris Asia system. In loop mode, 90% selectivity to alkenes was achieved at 90% PA and ByD conversion both with dissolved hydrogen and hydrogen gaseous flow, whereas only ca. 83% selectivity to the target product was achieved for DPA hydrogenation. H_2 and liquid flows, reaction temperature and substrate concentration obviously influence hydrogenation activity and selectivity. In flow-through mode, ca. 90% selectivity to BeD was achieved at over 90% ByD conversion. Hydrogenation activity and selectivity are also dependent on solution and H_2 flow as well as substrate concentration. Hydrogenation activity was well maintained and alumina beads kept good shape over the 100 h of hydrogenation, although some powder did fall from the support beads, leading to 22.7% Pd transfer from the catalyst beads into powder in the column reactor. However, no palladium leaching was detected in the reaction solution.

Acknowledgements

We gratefully acknowledge funding from the EU project MAPSYN (grant agreement No. CP-IP 309376, seventh Framework Program). We also thank Mrs. Laura Rotolo, Mr. Marco Bonito and Mr. Matteo Fornero for their pioneering investigations and the project partners from DSM (Basel, Switzerland) for their valuable cooperation.

References

1 M. Irfan, T. N. Glasnov and C. O. Kappe, *Chemsuschem*, 2011, **4**, 300–316.
2 R. R. Schrock and J. A. Osborn, *J. Am. Chem. Soc.*, 1976, **98**, 2143–2147.
3 M. W. van Laren and C. J. Elsevier, *Angew. Chem. Int. Ed.*, 1999, **38**, 3715–3717.
4 H. Lindlar, Hydrogenation of acetylenic bond utilizing a palladium-lead catalyst, U.S. Patent No. 2,681,938. 22 Jun. 1954.
5 H. Lindlar and R. Dubuis, *Org. Synth.*, 1966, 89–89.
6 J. G. Ulan, W. F. Maier and D. A. Smith, *J. Org. Chem.*, 1987, **52**, 3132–3142.
7 P. T. Witte, P. H. Berben, S. Boland, E. H. Boymans, D. Vogt, J. W. Geus and J. G. Donkervoort, *Top. Catal.*, 2012, **55**, 505–511.
8 B. Yang, R. Burch, C. Hardacre, P. Hu and P. Hughes, *Catal. Sci. Technol.*, 2017, **7**, 1508–1514.
9 S. O. Ojwach, A. O. Ogweno and M. P. Akerman, *Catal. Sci. Technol.*, 2016, **6**, 5069–5078.
10 Q. Zhang, J. Li, X. Liu and Q. Zhu, *Appl. Catal., A*, 2000, **197**, 221–228.
11 Y. Zhang, W. Diao, J. R. Monnier and C. T. Williams, *Catal. Sci. Technol.*, 2015, **5**, 4123–4132.

12 J. H. Kang, E. W. Shin, W. J. Kim, J. D. Park and S. H. Moon, *J. Catal.*, 2002, **208**, 310–320.
13 Y. Liu, Y. He, D. Zhou, J. Feng and D. Li, *Catal. Sci. Technol.*, 2016, **6**, 3027–3037.
14 J. Osswald, R. Giedigkeit, R. Jentoft, M. Armbruster, F. Girgsdies, K. Kovnir, T. Ressler, Y. Grin and R. Schlogl, *J. Catal.*, 2008, **258**, 210–218.
15 J. Kobayashi, Y. Mori, K. Okamoto, R. Akiyama, M. Ueno, T. Kitamori and S. Kobayashi, *Science*, 2004, **304**, 1305–1308.
16 J. H. Clark, *Green Chem.*, 1999, **1**, 1–8.
17 P. Anastas and N. Eghbali, *Chem. Soc. Rev.*, 2010, **39**, 301–312.
18 Z. Wu, E. Borretto, J. Medlock, W. Bonrath and G. Cravotto, *ChemCatChem*, 2014, **6**, 2762–2783.
19 Z. Wu, E. C. Gaudino, L. Rotolo, J. Medlock, W. Bonrath and G. Cravotto, *Chem. Eng. Process. Process Intensif.*, 2016, **110**, 220–224.
20 Z. Wu, G. Cravotto, E. C. Gaudino, A. Giacomino, J. Medlock and W. Bonrath, *Ultrason. Sonochem.*, 2017, **35**, 664–672.
21 P. Clark, M. Poliakoff and A. Wells, *Adv. Synth. Catal.*, 2007, **349**, 2655–2659.
22 R. Ciriminna, V. Pandarus, F. Béland and M. Pagliaro, *Catal. Sci. Technol.*, 2016, **6**, 4678–4685.
23 J. J. Bakker, M. M. Zieverink, R. W. Reintjens, F. Kapteijn, J. A. Moulijn and M. T. Kreutzer, *ChemCatChem*, 2011, **3**, 1155–1157.
24 Y. Önal, M. Lucas and P. Claus, *Chem. Eng. Technol.*, 2005, **28**, 972–978.
25 N. Yoswathananont, K. Nitta, Y. Nishiuchi and M. Sato, *Chem. Commun.*, 2005, 40–42.
26 D. Teschner, E. Vass, M. Havecker, S. Zafeiratos, P. Schnorch, H. Sauer, a Knopgericke, R. Schlogl, M. Chamam and a Wootsch, *J. Catal.*, 2006, **242**, 26–37.
27 F. Liguori and P. Barbaro, *J. Catal.*, 2014, **311**, 212–220.
28 G. Vilé, N. Almora-Barrios, S. Mitchell, N. Lopez and J. Perez-Ramirez, *Chem. Eur. J.*, 2014, **20**, 5926–5937.
29 G. Vilé, S. Wrabetz, L. Floryan, M. E. Schuster, F. Girgsdies, D. Teschner and J. Pérez-Ramírez, *ChemCatChem*, 2014, **6**, 1928–1934.
30 R. V. Jones, L. Godorhazy, N. Varga, D. Szalay, L. Urge and F. Darvas, *J. Comb. Chem.*, 2006, **8**, 110–116.
31 B. Desai and C. O. Kappe, *J. Comb. Chem.*, 2005, **7**, 641–643.
32 A. Kirschning, W. Solodenko and K. Mennecke, *Chem. Eur. J.*, 2006, **12**, 5972–5990.
33 T. Ouchi, C. Battilocchio, J. M. Hawkins and S. V. Ley, *Org. Process Res. Dev.*, 2014, **18**, 1560–1566.
34 M. O'Brien, N. Taylor, A. Polyzos, I. R. Baxendale and S. V. Ley, *Chem. Sci.*, 2011, **2**, 1250–1257.
35 E. V. Rebrov, E. A. Klinger, A. Berenguer-Murcia, E. M. Sulman and J. C. Schouten, *Org. Process Res. Dev.*, 2009, **13**, 991–998.
36 G. Vilé and J. Pérez-Ramírez, *Nanoscale*, 2014, **6**, 13476–13482.
37 J. Wegner, S. Ceylan and A. Kirschning, *Chem. Commun.*, 2011, **47**, 4583–4592.
38 G. Jas and A. Kirschning, *Chem. Eur. J.*, 2003, **9**, 5708–5723.
39 Z. Wu, N. Cherkasov, G. Cravotto, E. Borretto, A. O. Ibhadon, J. Medlock and W. Bonrath, *ChemCatChem*, 2015, **7**, 952–959.
40 Asia Flow Chemistry, https://syrris.com/product/asia-flow-chemistry/, 2017.

41 A. Sachse, N. Linares, P. Barbaro, F. Fajula and A. Galarneau, *Dalton Trans.*, 2013, **42**, 1378–1384.
42 E. Brunner, *J. Chem. Eng. Data*, 1985, **30**, 269–273.
43 T. Katayama and T. Nitta, *J. Chem. Eng. Data*, 1976, **21**, 194–196.
44 A. Borodzinski and G. C. Bond, *Catal. Rev.*, 2006, **48**, 91–144.
45 M. Garcıa-Mota, B. Bridier, J. Pérez-Ramírez and N. López, *J. Catal.*, 2010, **273**, 92–102.
46 D. Lennon, R. Marshall, G. Webb and S. Jackson, *Stud. Surf. Sci. Catal.*, 2000, **130**, 245–250.
47 N. A. Khan, S. Shaikhutdinov and H.-J. Freund, *Catal. Lett.*, 2006, **108**, 159–164.
48 G. Vilé, B. Bridier, J. Wichert and J. Pérez-Ramírez, *Angew. Chem. Int. Ed.*, 2012, **51**, 8620–8623.
49 D. Teschner, J. Borsodi, A. Wootsch, Z. Révay, M. Hävecker, A. Knop-Gericke, S. D. Jackson and R. Schlögl, *Science*, 2008, **320**, 86–89.
50 T. Nijhuis, G. van Koten and J. Moulijn, *Appl. Catal., A*, 2003, **238**, 259–271.
51 J. Alves, S. Bressa, O. Martınez and G. Barreto, *Chem. Eng. J.*, 2007, **125**, 131–138.
52 R. Nishio, M. Sugiura and S. Kobayashi, *Org. Biomol. Chem.*, 2006, **4**, 992–995.
53 R. D. Adams, T. S. Barnard, Z. Li, W. Wu and J. Yamamoto, *J. Am. Chem. Soc.*, 1994, **116**, 9103–9113.
54 H. H. Horváth, G. Papp, C. Csajági and F. Joó, *Catal. Commun.*, 2007, **8**, 442–446.
55 A. Kirschning, C. Altwicker, G. Dräger, J. Harders, N. Hoffmann, U. Hoffmann, H. Schönfeld, W. Solodenko and U. Kunz, *Angew. Chem. Int. Ed.*, 2001, **40**, 3995–3998.
56 A. Siva Reddy and K. C. Kumara Swamy, *Angew. Chem. Int. Ed.*, 2017, 56, 6984-6988.